

# DeepQTMT: A Deep Learning Approach for Fast QTMT-based CU Partition of Intra-mode VVC

Tianyi Li, Mai Xu *Senior Member, IEEE*, Runzhi Tang

**Abstract**—The latest standard Versatile Video Coding (VVC) significantly improves the coding efficiency over its ancestor standard High Efficiency Video Coding (HEVC), but at the expense of sharply increased complexity. In VVC, the quad-tree plus multi-type tree (QTMT) structure of coding unit (CU) partition accounts for most of encoding time, due to the brute-force search for recursive rate-distortion (RD) optimization. Instead of the brute-force QTMT search, this paper proposes a deep learning approach to predict the QTMT-based CU partition, for drastically accelerating the encoding process of intra-mode VVC. First, we establish a large-scale database containing sufficient CU partition patterns with diverse video content, which can facilitate the data-driven VVC complexity reduction. Next, we propose a multi-stage exit CNN (MSE-CNN) model with an early exit mechanism to determine the CU partition, in accord with the flexible QTMT structure at multiple stages. Then, we design an adaptive loss function for training the MSE-CNN model, synthesizing both the uncertain number of split modes and the target on minimized RD cost. Finally, a multi-threshold decision scheme is developed, achieving desirable trade-off between complexity and RD performance. Experimental results demonstrate that our approach can reduce the encoding time of VVC by 44.65%~66.88% with the negligible Bjøntegaard delta bit-rate (BD-BR) of 1.322%~3.188%, which significantly outperforms other state-of-the-art approaches.

**Index Terms**—Versatile Video Coding, complexity reduction, coding unit partition, deep learning

## I. INTRODUCTION

Along with the development of multimedia technology, ultra-high definition (UHD) and virtual reality (VR) video are increasingly widespread, causing the explosive growth of visual data. High Efficiency Video Coding (HEVC), as the current-generation standard, becomes gradually incapable for the future video market. Therefore, Joint Video Exploration Team (JVET) is developing the next-generation standard, i.e., Versatile Video Coding (VVC). For VVC, a variety of new coding techniques were adopted, such as the quad-tree plus multi-type tree (QTMT) structure of coding unit (CU) partition, the position dependent intra prediction, the affine motion compensation prediction and so on. These new techniques introduced in VVC achieve large gains over HEVC in coding efficiency. However, the complexity of VVC is also increased sharply. As measured in the reference software VTM [1], the encoding complexity of VVC at intra-mode is averagely 18 times higher than that of HEVC, making VVC far from

practical applications. Therefore, it is necessary to significantly reduce the complexity of VVC, while keeping the desirable coding efficiency.

During the past decade, numerous studies have contributed to the complexity reduction of HEVC, which is the ancestor to VVC. In HEVC, the CU partition consumes the most encoding time, and thus many approaches [2]–[7] aimed to simplify the CU partition for reducing the complexity of HEVC. Similarly, the more flexible CU partition structure of VVC accounts for a large proportion of encoding complexity, which can be simplified as studied in [8]–[15]. These studies can be classified into two categories: heuristic approaches and data-driven approaches. In heuristic approaches, some intermediate features of encoding, e.g., textural homogeneity/complexity and spatial correlation, were utilized to build statistical models about the CU partition. With these models, the redundant rate-distortion optimization (RDO) processes in the earlier quad-tree plus binary-tree (QTBT) [8]–[10] or the brand-new QTMT [11], [12] structure of CU partition can be skipped. In data-driven approaches, the CU partition can be automatically learned from sufficient data, addressing the drawback that heuristic approaches rely heavily on the handcrafted feature extraction. As a representative deep learning model, the convolutional neural network (CNN) is able to exploit the spatial correlation of textural content. For example, Jin *et al.* [13] and Wang *et al.* [14] utilized CNN models to determine the range of CU depth in the QTBT structure. The shortcoming of [13], [14] lies in only limited potential to reduce the encoding complexity, because various CU partition patterns may be with the same CU depth. Later, Galpin *et al.* [15] proposed directly deciding the CU partition, by predicting all possible CU boundaries in unit of  $4 \times 4$  blocks with a deep CNN. However, the bottom-up decision in [15] leads to redundant computation of CNN, for the most cases when split CUs do not reach the minimum CU size. Moreover, to the best of our knowledge, no existing data-driven approach is designed for the newest QTMT structure in VVC. Thus, it is worthwhile to directly determine the QTMT-based CU partition of VVC in a data-driven manner, benefiting from high prediction accuracy of deep learning.

In this paper, we propose a deep learning approach to accurately predict the CU partition, aiming at VVC complexity reduction at intra-mode. First, we establish a large-scale database for learning the QTMT-based CU partition in VVC<sup>1</sup>, collected from 8,000 raw images and 204 raw video sequences at four quantization parameter (QP) values. Analyzed from

T. Li, M. Xu and R. Tang are with the School of Electronic and Information Engineering, Beihang University, Beijing 100191, China.

M. Xu is also with the Hangzhou Innovation Institute, Beihang University, Hangzhou 310051, China.

Corresponding author: Mai Xu (MaiXu@buaa.edu.cn)

<sup>1</sup>Available online at: <https://github.com/tianyili2017/CPiV>

the sufficient data, we find that the possible split modes of CUs depend on the stage of CU partition and the CU size. Next, we propose a multi-stage exit CNN (MSE-CNN) model to determine the CU partition at multiple stages. Combining conditional convolution in the backbone and sub-networks in the branch, the MSE-CNN model is sufficient in network capacity to learn the CU partition. In addition, we introduce an early exit mechanism to drastically reduce the complexity of MSE-CNN, by skipping the prediction of redundant CUs. Furthermore, we design an adaptive loss function for training the MSE-CNN model, synthesizing both the classification loss with uncertain number of split modes and the target on minimized rate-distortion (RD) cost. Finally, a multi-threshold decision scheme is developed to achieve a desirable trade-off between complexity and RD performance. As a result, our approach can drastically reduce the complexity of intra-mode VVC, while keeping the RD performance. In brief, the main contributions of this paper are summarized as follow.

- We establish a large-scale database to learn the QTMT-based CU partition of intra-mode VVC, which may facilitate other data-driven VVC complexity reduction works.
- We propose a deep MSE-CNN model with an early exit mechanism to determine the CU partition at multiple stages, with little computation overhead.
- We design an adaptive loss function synthesizing both the variable number of split modes and the optimization on RD performance, for training our MSE-CNN model.

The rest of this paper is organized as follows. Section II reviews the related works on complexity reduction for VVC and its ancestors. Section III presents the database for the QTMT-based CU partition. In Section IV, we propose the MSE-CNN approach for fast CU partition in VVC. Section V shows the experimental results to verify the effectiveness of our MSE-CNN approach, and Section VI concludes this paper.

## II. RELATED WORKS

During the past decade, extensive approaches have been proposed to speed up the block partition for VVC and other video coding standards.

### A. Approaches for Previous Standards

Prior to the VVC standard, some main video coding standards include the HEVC, VP9 [16], AV1 [17] and AVS2 [18]. Among them, the HEVC standard developed by the Joint Collaborative Team on Video Coding (JCT-VC) has been established as the international video coding standard and become a research focus. The approaches for simplifying the coding tree unit (CTU) partition in HEVC can be generally classified into two categories: heuristic and data-driven approaches. Heuristic approaches extract intermediate features during encoding to build statistical models. With these models, the brute-force RDO search of CTU partition can be simplified, by skipping redundant processes in CTU partition. Considering that the CU partition consumes the most encoding time in HEVC, most approaches [2]–[5], [19]–[35]

focus on early deciding the CU partition. Specifically, Shen *et al.* [3] developed a dynamic CU depth range decision approach for fast intra-prediction, taking advantage of the texture property and coding information from the neighboring CUs. Then, texture homogeneity and spatial correlation are utilized to skip some CU sizes. Min *et al.* [23] proposed a fast CU partition prediction approach, in which global and local edge complexity is analyzed to decide the partition modes of CUs. In addition, the support vector machine (SVM), as an effective algorithm for classification, is utilized in fast CU partition. For example, Shen *et al.* [34] proposed modeling the early termination of CU partition as a binary-classification problem, in which a weighted SVM is utilized. Zhu *et al.* [5] proposed a binary and multi-class SVM approach to predict the CU partition with an off-on-line learning mechanism. In addition to the CU partition, other recursive processes nested in CTU can also be accelerated, such as prediction unit (PU) partition [25], [36], [37], PU mode selection [30], [38]–[40] and transform unit (TU) partition [25], [41].

While the heuristic approaches play a certain role in reducing the complexity of HEVC, they rely heavily on the handcrafted feature extraction. In fact, the features can be automatically learned from sufficient data, benefiting from recent success of deep learning. The CNN, as a representative deep learning model, has been utilized to reduce the complexity of CTU partition in [6], [7], [42], [43]. For example, Liu *et al.* [6] proposed a CNN approach for reducing the CU and PU searching modes, called the CTU structure decision CNN (CSD-CNN), such that the encoding process can be simplified. Laude *et al.* [43] formulated the intra-mode prediction as a multi-classification problem, and designed a five-layer CNN to select suitable prediction modes. Xu *et al.* [7] proposed a deep CNN model, i.e., the early-terminated hierarchical CNN (ETH-CNN), for predicting the structured output of CU partition. As a result, the complexity for HEVC can be significantly reduced. Compared with the heuristic approaches, data-driven approaches typically achieve higher prediction accuracy of CTU partition, beneficial for the overall complexity-RD performance. In addition to HEVC, heuristic and data-driven approaches also succeed in reducing the complexity of VP9 [44], [45], AV1 [46]–[48] and AVS2 [49]–[52], by learning the binary/ternary/quad-tree based block partition structure.

### B. Approaches for VVC

In VVC, the new partition structure of QTBT or QTMT is introduced, which further enhances the flexibility of CU partition but with extremely higher complexity. Similar to HEVC, the complexity of VVC can also be reduced by heuristic and data-driven approaches. For heuristic approaches [8]–[12], [53], [54], earlier ones were designed for the QTBT structure. Among them, Yamamoto [8] proposed a fast QTBT encoding method, which sets the different maximum binary-tree depth according to the temporal frame index. Wang *et al.* [9] proposed a fast QTBT decision approach, which utilizes a joint-classifier decision tree to early terminate unnecessary iterations. Amestoy *et al.* [10] adopted the random forest algorithm to early determine the QTBT partition. Later, the

QTMT structure has been introduced to VVC, and the corresponding approaches have emerged. Specifically, Fu *et al.* [11] proposed early skipping the vertical or horizontal CU partition with a Bayesian-based classifier. Lei *et al.* [54] developed a fast CU partition algorithm, which aims to skip redundant multi-type tree partition processes. Yang *et al.* [12] designed a low complexity CU partition pipeline by skipping unnecessary partition modes and intra-prediction processes. In [12], the CU partition is modeled as a multi-binary-classification process based on statistical analysis.

For data-driven approaches, Jin *et al.* [13] utilized a CNN to predict the range of CU depth in each  $32 \times 32$  CU, skipping the RDO search of unused CUs at intra-mode. Another CNN-based approach to predict CU depth range [14] can be used at inter-mode, which takes a residual CU as the CNN input because the partition depends on the correlation across different frames. Considering that various CU partition results may satisfy the same depth range, the models in [13], [14] can hardly predict the exact CU partition. Thus, they are limited in reducing the complexity of VVC. Later, Galpin *et al.* [15] proposed directly deciding the CU partition, by predicting all possible CU boundaries between adjacent  $4 \times 4$  blocks with a deep ResNet [55] model. However, the bottom-up decision in [15] leads to unnecessary calculation when a CTU is non-split or split into only a few large CUs.

In this paper, we propose a deep MSE-CNN approach to predict the CU partition for intra-mode VVC. Our approach differs from the existing ones in the following aspects. (1) Deep learning is utilized to automatically extract features from video content, instead of the handcrafted feature extraction in [11], [12], [54]. (2) Compared with the bottom-up CU boundary decision approach [15], our CNN model predicts the partition of larger CUs with former layers and that of smaller CUs with latter layers, i.e., multi-stage design. This enables the CNN to early exit and avoid redundant calculation. (3) Moreover, the existing data-driven approaches [13]–[15] for VVC were only designed for the QTBT structure of CU partition, while our approach satisfies the brand-new QTMT structure.

### III. CU PARTITION DATABASE

#### A. Overview of CU Partition

In this section, we briefly review the CU partition in the VVC standard, which is significantly different from that in the HEVC standard. In the HEVC standard, a CTU either contains a single CU or is recursively split into smaller square CUs via the quad-tree. The size of a CTU is  $64 \times 64$  pixels by default, and the minimize size of a CU can be  $8 \times 8$  in HEVC. In the VVC standard, the CU partition is more flexible than that in HEVC. Specifically, the CU partition structure evolves from the original structure of QTBT to QTMT, i.e., a CU can be split not only into squares, but also into rectangles using the QTMT structure. This enables the CUs of VVC adaptive to more texture patterns of video content. According to the QTMT structure, the CTU can either contain a single CU, or the CTU can be first split into smaller CUs with the quad-tree and then the smaller CUs can be split with the quad-tree

or multi-type tree. The multi-type tree includes the types of binary-tree and ternary-tree, which have two modes: horizontal and vertical modes. See Figure 1 for examples. Besides, the size of a CTU is  $128 \times 128$  by default, and the minimize size of a CU is  $4 \times 4$  in VVC. Consequently, the CU sizes in the CTU are diverse, ranging from  $128 \times 128$  to  $4 \times 4$ . Moreover, the CU partition for intra-mode VVC is separately applied for luminance and chrominance channels, different from intra-mode HEVC where the same CU partition is used for all color channels.<sup>2</sup> In summary, given the brand-new QTMT structure in VVC, both types and sizes for a CU are considerably more than those in HEVC.

For obtaining the split CUs with the above characteristics, there exists a multi-stage hierarchical partition process, as shown in Fig. 1. As can be seen in this figure, the process of splitting a  $128 \times 128$  CTU into  $64 \times 64$  CUs can be regarded as Stage 1. Then, the process of further splitting those  $64 \times 64$  CUs into  $32 \times 32$  CUs can be regarded as Stage 2, and so on. Among all 6 stages, only non-splitting and quad-tree modes are supported at Stages 1 and 2. For the subsequent stages, at most six modes are possible (i.e., non-splitting, quad-tree, horizontal binary-tree, vertical binary-tree, horizontal ternary-tree and vertical ternary-tree), satisfying the minimum width or height is 4 for CUs. Fig. 1 visualizes the possible CU sizes and split modes at different stages. In the VVC standard, the optimal CU partition result is obtained through a brute-force RDO search, by checking the RD cost of all possible CUs and then selecting the combination of CUs with the minimal RD cost. The basic idea of RDO search in VVC is similar to that in HEVC. However, the increased flexibility of CU partition in VVC leads to extremely higher coding complexity than HEVC. For each CTU in HEVC, 81 CUs need to be checked during encoding, while this number increases to 5,781 in VVC. In fact, only a small part of checked CUs (at least 1 CU, at most 1,024 CUs) exist in the final partition result. Therefore, a huge part of CUs can be skipped during the RDO search, through accurate prediction of CU partition.

#### B. Database Establishment

In order to train the models and evaluate the performance for our approach, we have established a large-scale database for the CU partition of intra-mode VVC (named as CPIV database). The data were collected from 204 raw video sequences [57]–[60] and 8,000 raw images [56] with multiple resolutions and diverse content. These video sequences and images were divided into three non-overlapping sets for training (6,400 images and 160 sequences), validation (800 images and 22 sequences) and test (800 images and 22 sequences). Among them, 182 training/validation sequences and all 8,000 images can be freely used for research without commercial purpose, and the details are listed in Table I. All video sequences and images were encoded by the VVC reference software VTM-7.0 [1]. Here, four QPs {22, 27, 32, 37} were

<sup>2</sup>In this section, we focus on the CU partition for luminance channel, as it consumes most of encoding time in the VTM encoder [1]. The CU partition for chrominance channel can be analyzed in a similar way, shown in the *Supporting Document*.

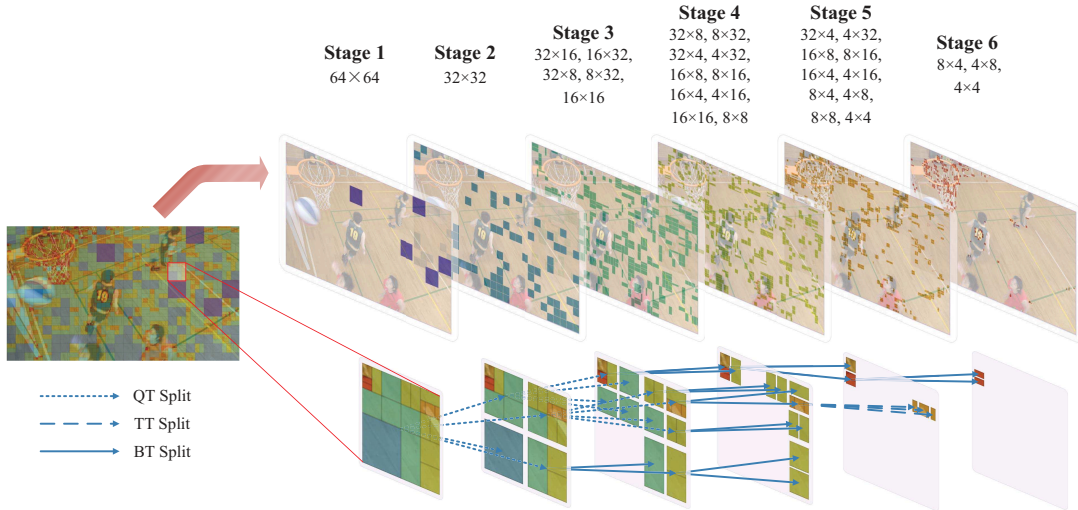


Fig. 1. Example of CU partition for luminance channel. The CUs split from different stages are distinguished by color.

TABLE I  
CONFIGURATION OF CPIV DATABASE

Source	Resolution	Num. of images/sequences	Total num. of CTUs	Total num. of CUs
Raw Image Dataset (RAISE) [56]	2880×1920	2,000	2,640,000	372,692,745
	2304×1536	2,000	1,728,000	242,719,640
	1536×1024	2,000	768,000	173,216,005
	768×512	2,000	192,000	58,271,751
Facial video [57]	1920×1080 (1080p)	6	72,960	9,660,712
Consumer Digital Video Library [58]	1920×1080 (1080p)	30	622,080	139,216,238
	640×360 (360p)	59	40,520	20,699,422
Xiph.org [59]	2048×1080 (2K)	18	95,232	21,108,370
	1920×1080 (1080p)	24	471,840	125,995,868
	1280×720 (720p)	4	30,600	15,913,824
	704×576 (4CIF)	5	12,400	5,411,228
	720×486 (NTSC)	7	10,545	4,765,478
	352×288 (CIF)	25	14,368	8,603,450
	352×240 (SIF)	4	688	753,882
Aggregated		8,182	6,699,233	1,199,028,613

applied to encode these sequences and images at the All-Intra (AI) configuration with the file *encoder\_intra\_vtm.cfg*. Considering that only resolutions in multiples of the minimum CU size (8×8 by default) are supported in VTM-7.0, the NTSC sequences were cropped to 720×480 by removing the bottom edges of the frames. Moreover, the sequences longer than 10 seconds were clipped to be 10 seconds, avoiding over-large video files in our database.

For our CPIV database, the CU partition labels can be obtained after encoding. Each label represents the ground-truth split mode for a CU, equal to one of six possible split modes, i.e., non-splitting (mode 0), quad-tree (mode 1), horizontal binary-tree (mode 2), vertical binary-tree (mode 3), horizontal ternary-tree (mode 4) and vertical ternary-tree (mode 5). In addition, the RD cost for all possible modes of each CU were recorded, which can be used for network training, in accord with the target of optimizing RD in VVC. Then, each CTU with the corresponding partition labels and RD cost of its CUs, forms a sample in the CPIV database. As shown in Table I, the CPIV database contains 6,699,233 samples with more than 1 billion CUs in total, providing sufficient data for training our

MSE-CNN model. For more detailed analysis, the proportions of CUs with different split modes<sup>3</sup> are illustrated in Fig. 2. It indicates that the number of possible modes depends on the specific CU size, ranging from 2 to 6, which conforms to the CU partition rules mentioned in Section III-A. Also, the proportions of different split modes are highly unbalanced. For example, ternary-tree split CUs, i.e., modes 4 and 5, account for less than 15% for all CU sizes, while non-splitting CUs, i.e., mode 0, are predominant for most CU sizes. Thus, the multi-stage CU partition problem is more sophisticated than a typical image classification problem with only one output and balanced classes. To solve this problem, the next section focuses on the elaborated MSE-CNN model, adaptive to the QTMT-based CU partition in the VVC standard.

#### IV. COMPLEXITY REDUCTION FOR VVC INTRA-MODE

##### A. MSE-CNN for Learning CU Partition

In this section, we present the proposed MSE-CNN model for learning the QTMT-based CU partition in VVC. For the standard VVC encoder, all possible CUs in each CTU should be checked in a bottom-up manner, using the brute-force RDO search. In our approach, the CU partition can be predicted by MSE-CNN in a stage-wise top-down manner, in order to drastically accelerate the encoding process. The overall structure of MSE-CNN is shown in Figure 3-(a). As shown in this figure, the luminance channel of a 128×128 CTU is input to MSE-CNN, and flows through a convolutional layer to extract a group of 128×128 feature maps. Using the feature maps, at most six split mode decision units are successively applied, corresponding to the CU partition at six stages. In each split mode decision unit, the input feature maps first flow through a series of convolutional layers, named as conditional convolution, to extract textural features in the backbone of MSE-CNN. Then, the feature maps are fed into a sub-network

<sup>3</sup>In the VTM-7.0 encoder, all 128×128 CTUs are forced to be split into 64×64 CUs by quad-tree. As a fixed stage, it does not need to be learned. Thus, our analysis focuses on 64×64 and smaller CUs.

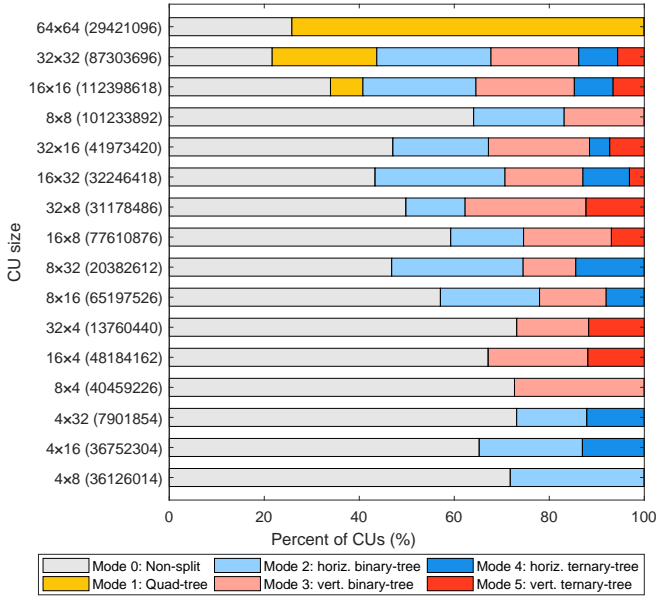


Fig. 2. Proportions of CUs with different split modes for luminance channel. Note that each value inside parentheses represents the number of CUs.

to predict the split mode of one CU, conducted in the branches of MSE-CNN. If the prediction result is non-split, the CU partition is early-terminated at the current stage; otherwise, the part of feature maps, corresponding to the location of each split CU, is input to the next stage. The details about conditional convolution and sub-network are presented below.

**Conditional convolution.** The efficacy of a neural network relies on sufficient features and depth. Therefore, we extract textural features and deepen the MSE-CNN model in this process. Instead of a fixed structure, we select the structure on condition of the CU size. It is because the CU size may be considerably variable at the same stage, and different depth of extracted features tend to be suitable for them. The mechanism of conditional convolution is shown in Figure 3-(b), which is inspired by the efficient ResNet model [55]. Assume that the size of CU is  $w \times h$ . The minimal axis length of CU is  $\min(w, h)$ , and it is used to measure the granularity of CU partition. If the minimal axis length of current CU and that of its parent CU are  $a_c$  and  $a_p$ , respectively, the input feature maps are processed with  $n_r \in \{0, 1, 2\}$  residual units, formulated as

$$n_r = \begin{cases} \log_2 \left( \frac{a_p}{a_c} \right) & 4 \leq a_c \leq 64 \\ 1 & a_c = 128. \end{cases} \quad (1)$$

Here, the convolution operations in residual units are all overlapping with stride of 1 and zero-padding, keeping the size of feature maps unchanged. Afterwards, the feature maps processed by  $n_r$  residual units are used as input to the sub-network. Such unfixed design provides a crucial property for MSE-CNN, i.e., the index of residual unit  $k \in \{1, 2, \dots, 6\}$  is determinate once the size of the current CU is known, satisfying  $k = \log_2 \left[ \frac{256}{\min(w, h)} \right]$ . For all residual units with the same index  $k$  (though they may be at different stages), we need to share the trainable parameters, ensuring that all similar-sized

CUs are fed with the same sorts of features in the following sub-network.

**Sub-network.** In each sub-network for the partition of  $64 \times 64$  or smaller CUs, the input feature maps flow into a series of convolutional and fully connected layers, for predicting the split mode. The configuration of each sub-network is related to its corresponding CU size, as shown in Figure 3-(b). In each sub-network, the input feature maps are fed into two or three convolutional layers, to extract low-level features for the CU partition. For all convolutional layers, the width and height of their kernels are integer powers of 2, e.g.,  $2 \times 2$  and  $4 \times 4$ . Also, the kernel strides in two dimensions are set equal to the width and height of the kernels, and thus all kernels are non-overlapping. Such non-overlapping convolution is adaptive to the size and location of non-overlapping CUs in the final partition. Then, the output feature maps of convolutional layers flow through two fully connected layers to obtain the split mode. Consequently, the output is the prediction of one-hot vector corresponding to the ground-truth split mode. Here, the output vector length ranges from 2 to 6, depending on the CU size. Moreover, QP also has a significant influence on the CU partition. Along with QP decreases, more CUs tend to be split, and vice versa. Therefore, before the first convolutional and the first fully connected layer, QP is supplemented as an external feature. Considering that some certain features in MSE-CNN may be related to QP, we apply a half-mask operation to these features, i.e., multiplying half of feature maps/vectors by the normalized QP value. As such, the MSE-CNN model is able to learn the CU partition at various QP values. Finally, the output of sub-network controls the following CU partition process. If the CU is predicted as non-split, the partition process early exits at the current stage; otherwise, the output of conditional convolution at the current stage is fed into the next stage.

As discussed above, the multi-stage design combining conditional operation and sub-networks can efficiently determine the QTMT-based CU partition for the VVC standard. In addition, the early-exit mechanism also drastically reduces the overall complexity of MSE-CNN, by skipping the prediction of redundant CUs. The experimental results of complexity reduction by our MSE-CNN approach is to be verified in Section V-B.

### B. Loss Function for Training MSE-CNN

Compared with a typical classification problem, the proposed MSE-CNN is more sophisticated with three main properties as follows.

- (I) The split modes depend on the corresponding CU size, with their numbers ranging from 2 to 6. More details are discussed in Section III.
- (II) There exist highly unbalanced proportions for different split modes. See Fig. 2 for more details.
- (III) In VVC, different split modes typically lead to different RD cost, while a simple cross-entropy function cannot address it.

Thus, the loss function for MSE-CNN model should be adaptive to the above properties.

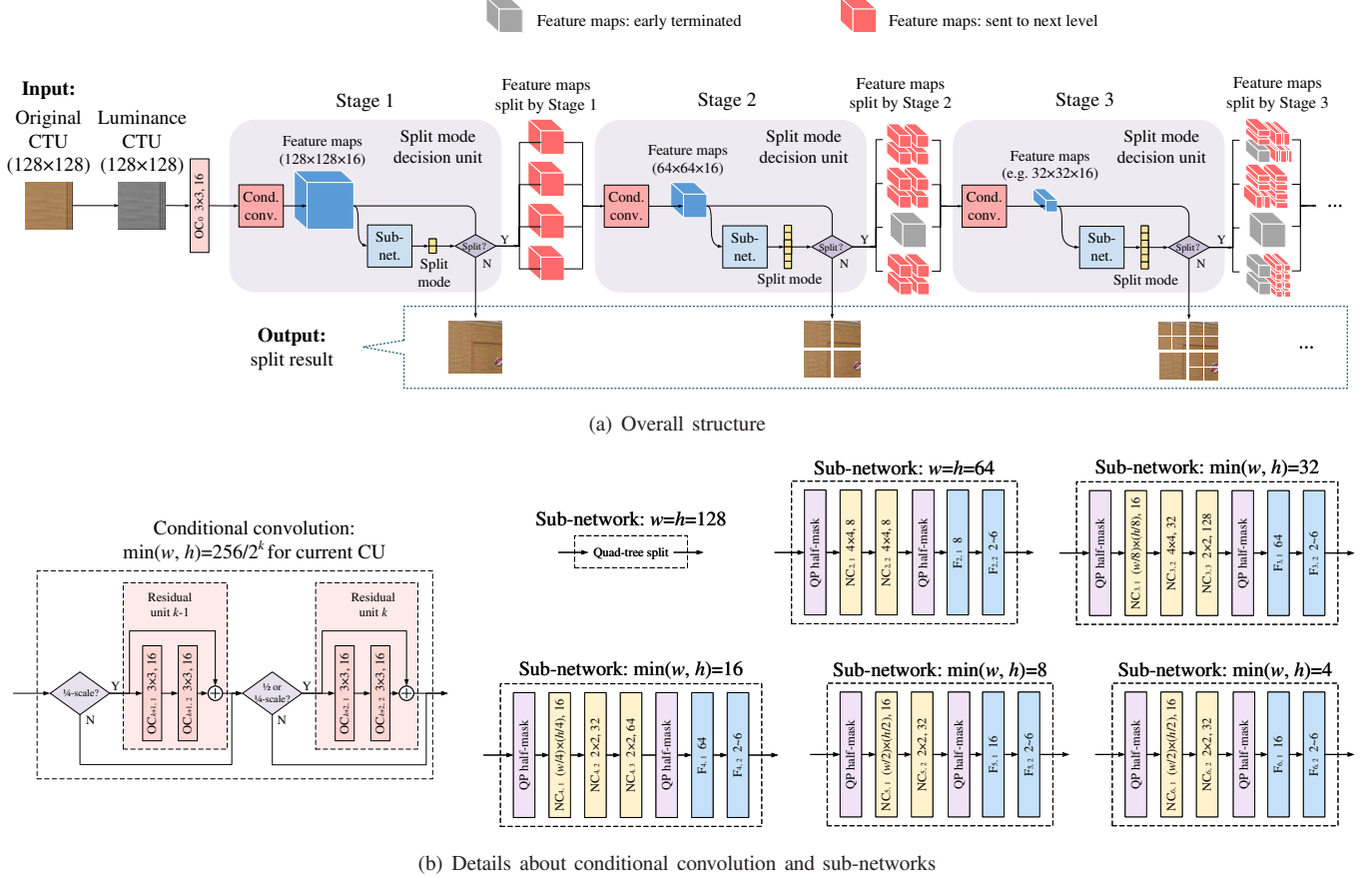


Fig. 3. Structure of MSE-CNN. The layer names started with OC, NC and F denote overlapping convolutional, non-overlapping convolutional and fully connected layers, respectively. For convolutional layers, “ $w_k \times h_k, n_k$ ” represents  $n_k$  output feature maps with kernel width of  $w_k$  and kernel height of  $h_k$ . For fully connected layers, the value after layer name is the number of output features. Note that all convolutional and fully connected layers are activated by the parametric rectified linear units (PReLU) [61], except the last fully connected layer in each sub-network activated by the Softmax function.

For a CU with width  $w$  and height  $h$ , the set of all candidate split modes is denoted by  $\mathcal{M}(w, h)$ . Each element  $m$  in  $\mathcal{M}(w, h)$  is the index of a split mode, where  $m \in \{0, 1, 2, 3, 4, 5\}$ . For ease of training, a mini-batch only contains CUs with the same size. Assume that the size of mini-batch is  $N$ , and the index of a CU is  $n$ . First, we apply the basic cross-entropy as the loss function:

$$L_{CE,B} = -\frac{1}{N} \sum_{n=1}^N \sum_{m \in \mathcal{M}} y_{n,m} \log(\hat{y}_{n,m}), \quad (2)$$

where  $y_{n,m}$  and  $\hat{y}_{n,m}$  represent the ground-truth binary label and predicted probability for the  $n$ -th CU at split mode  $m$ .

Considering the unbalanced proportions of split modes, different penalty weights can be applied to (2) according to the proportions. Then, the cross-entropy can be modified as

$$L_{CE} = -\frac{\sum_{n=1}^N (\frac{1}{p_m})^\alpha \cdot \sum_{m \in \mathcal{M}} y_{n,m} \log(\hat{y}_{n,m})}{\sum_{n=1}^N (\frac{1}{p_m})^\alpha}, \quad (3)$$

where  $p_m$  is the quantitative proportion of CUs with split mode  $m$ , satisfying  $\sum_{m \in \mathcal{M}} p_m = 1$ . Additionally,  $\alpha \in [0, 1]$  is an adjustable scalar to determine the importance of penalty weights. Here,  $\alpha = 0$  means that no penalty is applied according to  $\{p_m\}_{m \in \mathcal{M}}$ ; in this case, the MSE-CNN model

may be ill-trained, because the model tends to predict only the most-frequent split mode. In contrast,  $\alpha = 1$  indicates that each penalty weight is proportional to the inverse of  $p_m$ , avoiding the ill-trained MSE-CNN model. However, such setting can hardly learn the prior distribution of different split modes, and this may lead to low prediction accuracy. As a trade-off between prediction accuracy and reliability,  $\alpha \in (0, 1)$  is practically used. In our experiments,  $\alpha = 0.3$  was chosen by tuning over the validation set of our CPIV database. For more details about the hyper-parameter setting, see the section of experiments.

In (3), properties I and II are both addressed, while property III can be further considered by introducing a loss function of the RD cost, formulated as

$$L_{RD} = \frac{1}{N} \sum_{n=1}^N \sum_{m \in \mathcal{M}} y_{n,m} \left( \frac{r_{n,m}}{r_{n,\min}} - 1 \right), \quad (4)$$

where  $r_{n,m}$  is the RD cost for the  $n$ -th CU at split mode  $m$ , and  $r_{n,\min}$  is the minimum RD cost for this CU among all possible split modes. In the above equation,  $(\frac{r_{n,m}}{r_{n,\min}} - 1)$  can be seen as the normalized RD cost. The term  $y_{n,m} (\frac{r_{n,m}}{r_{n,\min}} - 1)$  punishes more on either larger wrongly-predicted probability  $y_{n,m}$  or larger RD cost  $r_{n,m}$ , in accord with the target of RD

optimization in VVC. Combining (3) and (4), the overall loss function for MSE-CNN is

$$L = L_{CE} + \beta \cdot L_{RD}, \quad (5)$$

where  $\beta$  is a positive scalar determining the importance of the RD cost. As a result, the MSE-CNN model can be properly trained by minimizing  $L$  of (5).

### C. Multi-threshold decision for MSE-CNN

Ideally, the whole CU partition is predicted by the proposed MSE-CNN model, such that all redundant checking of CUs in the original RDO process can be skipped to reduce the encoding complexity. However, the MSE-CNN model also introduces some wrongly predicted CU partition, leading to a degradation of RD performance. Therefore, we propose a multi-threshold decision scheme to achieve a trade-off between encoding complexity and RD performance.

In our multi-threshold decision scheme, a combination of decision thresholds  $\{\tau_s\}_{s=2}^6$ , with  $\tau_s$  ranging in  $[0, 1]$ , is applied on all stages of MSE-CNN, where  $s$  denotes the index of stage. Recall that  $\hat{y}_{n,m}$  represents the predicted probability for the  $n$ -th CU in a mini-batch with split mode  $m$ , where  $m$  is chosen from the candidate mode set  $\mathcal{M}$ . In the current VTM encoder, Stage 1 is deterministic and does not need to be predicted by MSE-CNN; thus, the multi-threshold values start from Stage 2. Let the highest predicted probability be  $\hat{y}_{n,\max} = \max_{m \in \mathcal{M}} \{\hat{y}_{n,m}\}$ . For all candidate modes  $m \in \mathcal{M}$  of this CU, only the modes with probability  $\hat{y}_{n,m} \geq \tau_s \cdot \hat{y}_{n,\max}$  are checked in the RDO process of the encoder, while other modes are early skipped. As such, threshold  $\tau_s$  controls the confidence of MSE-CNN prediction.

For the most aggressive setting,  $\tau_s = 1$  indicates that the split modes of all CUs are determined by the MSE-CNN model, as only the mode with  $\hat{y}_{n,m} = \hat{y}_{n,\max}$  is selected for the RDO process. This setting achieves the least encoding complexity but the most degradation on RD performance. In contrast,  $\tau_s = 0$  means that all CUs are checked by the original RDO process, where the encoding complexity is not reduced with no RD degradation. As a trade-off, threshold  $\tau_s$  is typically set between 0 and 1 in practice. Next, we provide a scheme for selecting  $\{\tau_s\}_{s=2}^6$  at the different stages of MSE-CNN, considering the unequal prediction accuracy of these stages. Figure 4 shows the prediction accuracy of MSE-CNN with the change of  $\tau_s$ , averaged over all 800 images and 22 video sequences in our CPIV database (See Section V for more details about the settings). For different stages and CU sizes, the number of possible split modes may be variable (i.e., the MSE-CNN model solves a classification problem with different numbers of classes), and thus the values of Figure 4 are in top-half accuracy. From this figure, we can see that Stage 2 always achieves the best prediction accuracy. For Stage 6, it has the second-best prediction accuracy when thresholds  $\{\tau_s\}_{s=2}^6$  are large, while it performs relatively worse when thresholds  $\{\tau_s\}_{s=2}^6$  are close to 0. For other stages, the difference of accuracy is insignificant. Accordingly, the multi-threshold values can be chosen in the following

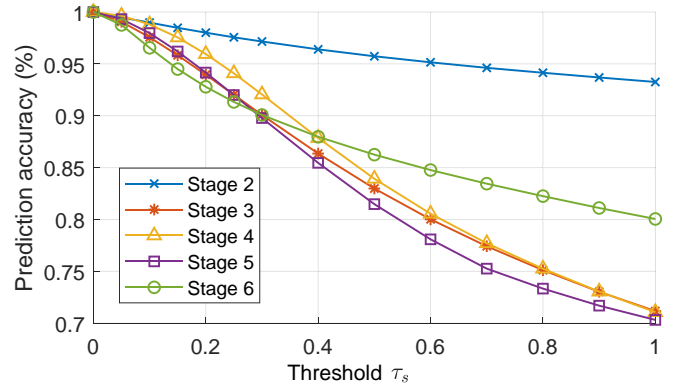


Fig. 4. Prediction accuracy of MSE-CNN on the validation data.

strategies, ensuring the overall prediction accuracy of MSE-CNN.

- Case 1 (more time saving): if average threshold  $\frac{1}{5} \sum_{s=2}^6 \tau_s \geq 0.4$ , then  $\tau_2 \geq \tau_6 \geq \tau_3 \approx \tau_4 \approx \tau_5$ .
- Case 2 (better RD performance): if average threshold  $\frac{1}{5} \sum_{s=2}^6 \tau_s < 0.4$ , then  $\tau_2 \geq \tau_4 \approx \tau_3 \approx \tau_5 \geq \tau_6$ .

## V. EXPERIMENTAL RESULTS

In this section, we conduct experiments to evaluate the effectiveness of our approach in reducing the complexity of intra-mode VVC. Section V-A presents the experimental settings of our approach. Section V-B evaluates the complexity and RD performance by comparing our approach with three state-of-the-art approaches [7], [11], [12]. Section V-C analyzes the running time of our approach.

### A. Configuration and settings

**Configuration of experiments.** In our experiments, all complexity reduction approaches were implemented in the VVC reference software VTM 7.0 [1]. The experiments were evaluated on all 22 video sequences of Classes A~E in the JVET test set [60]. They were encoded at the AI configuration (using the file *encoder\_intra\_vtm.cfg*) at four QP values  $\{22, 27, 32, 37\}$ . After encoding,  $\Delta T$ , which denotes the time-saving rate of encoding compared over the original VTM, was recorded to measure the complexity reduction. In addition, the Bjøntegaard delta bit-rate (BD-BR) and Bjøntegaard delta PSNR (BD-PSNR) [62] were used to assess the RD performance. All experiments were conducted on a computer with an Intel(R) Xeon(R) CPU E5-2650 v3 @ 2.30GHz, 128 GB RAM and the Ubuntu 18.04 64-bit operating system. Note that a GeForce RTX 2080 Ti GPU was used to accelerate the training speed, but it was disabled when testing the encoding performance for fair comparison.

**Settings for MSE-CNN.** In intra-mode VVC, the CU partition for luminance and chrominance is determined separately by default. Thus, we trained the MSE-CNN models on different color channels separately. In total, 19 MSE-CNN models were trained according to both CU size and color channel. Figure 5 illustrates the sequences of different MSE-CNN models and the trainable components in each model.

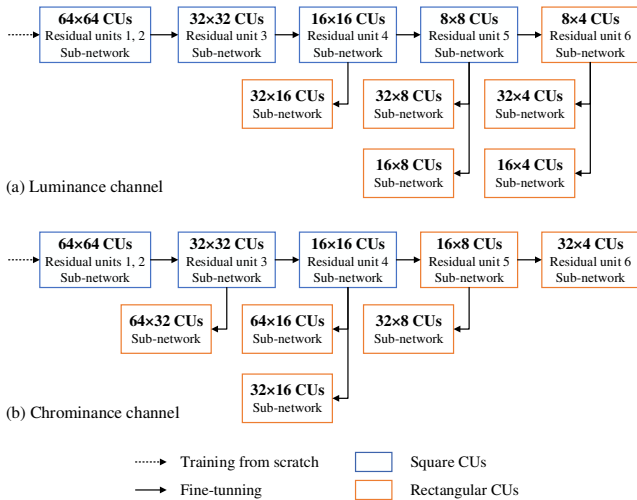


Fig. 5. Training process of MES-CNN. Each block represents the training for each model.

TABLE II  
MULTI-THRESHOLD VALUES FOR MSE-CNN

Setting	Threshold values					Average
	$\tau_2$	$\tau_3$	$\tau_4$	$\tau_5$	$\tau_6$	
(i)	0.75	0.55	0.55	0.55	0.6	0.6
(ii)	0.65	0.45	0.45	0.45	0.5	0.5
(iii)	0.5	0.4	0.35	0.35	0.4	0.4
(iv)	0.45	0.3	0.25	0.25	0.25	0.3
(v)	0.3	0.2	0.2	0.15	0.15	0.2

Here, all rectangular CUs fed into these models were with the width larger than the height. For any CU with height larger than width, it needed to be transposed in advance, in terms of both content and partition patterns. For training MSE-CNN, all hyper-parameters were tuned on the validation set of the CPIV database. Specifically, we set  $\alpha$  and  $\beta$  to be 0.3 and 1.0 in the loss function of MSE-CNN, respectively. When training from scratch, all weight and bias parameters were randomly set with the Xavier initialization [63]. For each model trained from scratch or fine-tuning, 500,000 iterations were conducted, with the batch size of 32. The learning rate was initially set to  $10^{-4}$  and then decreased by 1% exponentially every 2,000 iterations. During this process, the parameters in trainable components were optimized with the Adam algorithm [64], while the other parameters remained unchanged. In the inference phase of MSE-CNN, five settings of multi-threshold values were chosen according to the analysis in Section IV-C, as shown in Table II. Among them, Settings (ii) and (iv) are typical circumstances for Cases 1 and 2 of the multi-threshold scheme, respectively, which are detailed in the next-subsection. Other three settings are also analyzed, in terms of the overall performance.

### B. Performance evaluation

In this section, we evaluate the performance in both complexity reduction and coding efficiency, by comparing our MSE-CNN approach with other state-of-the-art approaches

[7], [11], [12]. Among them, our approach and [11], [12] are all designed for the brand-new QTMT-based CU partition structure in VVC. In addition, we also tested a deep-learning-based approach [7] for HEVC complexity reduction, through transferring it to the VVC standard. Table III demonstrates the comparative results on all 22 test video sequences. We can see from Table III that Setting (ii) of our approach averagely reduces 59.57%~66.88% of encoding time on the video sequences, more effective than the time reduction of 55.65%~59.14% in [11], 52.48%~64.44% in [12] and 38.19%~41.79% in [7]. For RD performance, Setting (iv) of our approach achieves the least BD-BR redundancy of 1.322% and BD-PSNR degradation of 0.055dB on average, better than all state-of-the-art approaches [7], [11], [12]. Moreover, for any state-of-the-art approach, there always exists one setting of our approach better than it on both encoding time and RD performance, i.e., Setting (ii) outperforming [11], [12] and Setting (iv) outperforming [7] in terms of all three metrics  $\Delta T$ , BD-BR and BD-PSNR. Such comparison verifies that our approach is with the best overall complexity-RD performance on video sequences. It is because the data-driven MSE-CNN model in our approach can directly predict the CU partition with high accuracy, which helps to skip most redundant processes in the RDO search. In addition, the change of performance across video sequences is insignificant in our approach. The standard deviation of  $\Delta T$ , BD-BR and BD-PSNR are within 8.81%, 0.915% and 0.044dB, respectively, smaller than or comparative to other approaches. As a result, our approach holds the outperformance on most video sequences at most QP values.

For a more comprehensive analysis, Figure 6 depicts the complexity-RD performance of different approaches, averaged over all four QP values. Note that the curve of our approach is obtained by varying the multi-threshold values mentioned in Section V-A. As shown in this figure, the curve of our approach locates to the bottom-left of all other approaches. It indicates that our approach can always save more encoding time under the same BD-BR value, or in other words, keep better RD performance with the same encoding time. Therefore, the effectiveness of our approach has been verified, which also provides various trade-off between encoding time and RD performance.

### C. Running time analysis

To efficiently accelerate VVC encoding, it is required that the approach itself consumes little time overhead. Thus, we analyze the running time of our deep MSE-CNN model, by comparing it over the original VTM 7.0 encoder [1]. Figure 7 shows the ratio of time for the MSE-CNN model and that for other parts in encoding. The results are averaged over all test sequences with the same resolution at all four QP values. From this figure, we can find that the time overhead introduced by MSE-CNN is less than 5% for most resolutions, compared over the original VTM. The average time overhead is 3.67%, which accounts for only a small part of the total encoding time. It is because the early-exit mechanism in MSE-CNN can skip most redundant checking processes in the QTMT-based



TABLE III  
COMPLEXITY-RD PERFORMANCE ON VIDEO SEQUENCES

Class	Sequence	Approach	BD-BR (%)	BD-PSNR (dB)	$\Delta T$ (%)			
					QP=22	QP=27	QP=32	QP=37
A1	Campfire	[11]	4.328	-0.120	-62.42	-61.36	-62.07	-60.85
		[12]	2.876	-0.072	-51.80	-57.84	-57.84	-35.33
		[7]	<b>1.655</b>	<b>-0.046</b>	-35.69	-38.64	-40.36	-35.59
		Our (ii)	4.165	-0.116	<b>-65.74</b>	<b>-68.21</b>	<b>-68.02</b>	<b>-64.12</b>
	Our (iv)	2.015	-0.056	-43.70	-47.20	-52.10	-51.74	
	FoodMarket4	[11]	2.349	-0.077	-61.71	-55.05	-52.29	-44.26
		[12]	3.454	-0.124	-60.36	<b>-67.47</b>	-61.65	<b>-51.72</b>
		[7]	2.254	-0.073	-35.96	-27.32	-33.50	-34.31
		Our (ii)	2.784	-0.091	<b>-68.78</b>	-61.97	<b>-56.56</b>	-44.31
	Our (iv)	<b>1.256</b>	<b>-0.042</b>	-49.19	-44.09	-42.08	-33.58	
	Tango2	[11]	3.367	-0.047	-65.30	-59.38	-49.90	-35.29
		[12]	6.852	-0.136	-51.42	<b>-72.07</b>	-22.70	-29.24
[7]		2.604	-0.046	-34.14	-34.69	-38.63	<b>-36.28</b>	
Our (ii)		3.485	-0.051	<b>-70.83</b>	-66.65	<b>-53.02</b>	-26.91	
Our (iv)	<b>1.521</b>	<b>-0.024</b>	-52.61	-50.06	-39.91	-20.53		
A2	CatRobot1	[11]	6.748	-0.152	-61.81	-61.95	-59.75	-55.49
		[12]	5.266	-0.146	-53.00	-62.05	-40.30	-40.55
		[7]	<b>1.484</b>	<b>-0.039</b>	-32.25	-20.74	-36.13	-33.63
		Our (ii)	4.875	-0.112	<b>-69.08</b>	<b>-64.90</b>	<b>-61.40</b>	<b>-56.11</b>
	Our (iv)	2.163	-0.053	-49.40	-45.80	-43.39	-43.03	
	DaylightRoad2	[11]	2.796	-0.064	-63.00	-61.36	-61.17	-57.58
		[12]	7.968	-0.149	-59.76	<b>-71.35</b>	-56.03	<b>-64.67</b>
		[7]	1.166	-0.045	-40.94	-31.71	-23.12	-27.92
		Our (ii)	2.781	-0.067	<b>-72.54</b>	-68.06	<b>-63.65</b>	-58.25
	Our (iv)	<b>1.163</b>	<b>-0.030</b>	-56.51	-49.62	-45.93	-45.35	
	ParkRunning3	[11]	2.687	-0.133	<b>-64.87</b>	<b>-62.54</b>	<b>-62.40</b>	-61.80
		[12]	3.167	-0.140	-50.18	-57.20	-36.12	-52.14
[7]		<b>0.918</b>	<b>-0.045</b>	-23.22	-24.65	-33.86	-34.51	
Our (ii)		2.675	-0.132	-60.50	-60.47	<b>-62.09</b>	<b>-68.97</b>	
Our (iv)	1.146	-0.056	-35.59	-36.27	-41.64	-53.20		
B	MarketPlace	[11]	2.004	-0.076	-61.55	-60.73	-59.32	-58.32
		[12]	3.286	-0.122	-51.66	<b>-68.29</b>	-43.56	-63.12
		[7]	1.166	-0.045	-23.14	-35.44	-34.33	-40.13
		Our (ii)	1.891	-0.072	<b>-64.84</b>	-64.42	<b>-65.38</b>	<b>-65.97</b>
	Our (iv)	<b>0.803</b>	<b>-0.031</b>	-41.60	-43.42	-47.78	-53.72	
	RitualDance	[11]	3.859	-0.183	-58.74	-58.32	-57.22	-54.40
		[12]	4.053	-0.191	-60.39	<b>-70.14</b>	-49.14	-58.13
		[7]	1.550	-0.075	-16.47	-24.19	-41.36	-38.64
		Our (ii)	2.693	-0.129	<b>-67.20</b>	-64.29	<b>-61.78</b>	<b>-58.64</b>
	Our (iv)	<b>1.071</b>	<b>-0.052</b>	-46.39	-44.97	-43.61	-44.51	
	BasketballDrive	[11]	3.553	-0.091	-59.71	-61.18	-60.12	-54.79
		[12]	5.923	-0.148	-56.33	-70.28	-55.24	-59.31
[7]		<b>1.595</b>	<b>-0.042</b>	-37.79	-39.95	-41.65	-36.07	
Our (ii)		3.873	-0.101	<b>-71.39</b>	<b>-72.16</b>	<b>-67.86</b>	<b>-62.60</b>	
Our (iv)	1.642	-0.044	-52.95	-55.62	-51.52	-48.03		
BQTerrace	[11]	1.750	-0.074	-49.61	-58.27	-57.78	-58.01	
	[12]	4.378	-0.177	-48.89	<b>-70.15</b>	-67.68	-63.55	
	[7]	1.459	-0.066	-22.34	-48.56	-49.64	-50.20	
	Our (ii)	2.574	-0.123	<b>-54.21</b>	-69.53	<b>-67.74</b>	<b>-66.09</b>	
Our (iv)	<b>1.111</b>	<b>-0.054</b>	-29.37	-51.23	-50.41	-51.45		
Cactus	[11]	3.541	-0.112	-60.10	-60.11	-58.78	-59.22	
	[12]	4.555	-0.143	-57.75	-67.39	-61.31	-62.65	
	[7]	1.304	-0.042	-41.36	-41.55	-43.73	-40.13	
	Our (ii)	2.846	-0.091	<b>-69.85</b>	<b>-68.32</b>	<b>-66.23</b>	<b>-66.40</b>	
Our (iv)	<b>1.124</b>	<b>-0.036</b>	-49.41	-49.07	-47.60	-51.14		
C	BasketballDrill	[11]	4.285	-0.194	-56.73	-60.37	-59.61	-56.83
		[12]	4.596	-0.208	-58.17	<b>-62.68</b>	<b>-63.21</b>	-53.45
		[7]	1.744	-0.080	-41.90	-45.66	-44.42	-41.05
		Our (ii)	4.722	-0.212	<b>-63.15</b>	-61.55	-60.85	<b>-58.35</b>
	Our (iv)	<b>1.625</b>	<b>-0.074</b>	-40.14	-37.83	-39.26	-39.93	
	BQMall	[11]	4.193	-0.213	-59.27	-58.68	-59.18	-58.51
		[12]	4.975	-0.251	-61.97	-67.25	-64.64	-59.23
		[7]	<b>1.143</b>	<b>-0.058</b>	-43.95	-43.91	-43.26	-40.17
		Our (ii)	3.102	-0.158	<b>-70.67</b>	<b>-68.22</b>	<b>-65.89</b>	<b>-65.01</b>
	Our (iv)	1.170	-0.060	-52.86	-50.51	-46.87	-48.78	
	PartyScene	[11]	1.939	-0.130	-56.10	-57.26	-58.02	-59.28
		[12]	2.238	-0.152	-63.59	<b>-66.90</b>	<b>-67.57</b>	-52.39
[7]		0.779	-0.052	-44.89	-45.95	-47.78	-48.00	
Our (ii)		1.857	-0.124	<b>-65.70</b>	-66.15	-64.20	<b>-62.50</b>	
Our (iv)	<b>0.612</b>	<b>-0.041</b>	-47.29	-47.52	-43.70	-42.27		
RaceHorses	[11]	3.181	-0.171	-60.73	-58.76	-58.39	-57.71	
	[12]	2.746	-0.146	-57.22	-60.90	-54.99	-51.40	
	[7]	0.997	-0.054	-44.81	-41.90	-45.77	-44.66	
	Our (ii)	2.503	-0.135	<b>-66.89</b>	<b>-65.12</b>	<b>-63.40</b>	<b>-67.31</b>	
Our (iv)	<b>0.963</b>	<b>-0.052</b>	-47.36	-44.07	-42.93	-51.42		
D	BasketballPass	[11]	3.380	-0.198	-59.82	-58.51	-58.02	-56.73
		[12]	2.914	-0.169	-51.80	-55.80	-50.54	-44.78
		[7]	<b>0.898</b>	<b>-0.053</b>	-41.25	-41.03	-41.44	-39.32
		Our (ii)	3.664	-0.214	<b>-66.22</b>	<b>-64.96</b>	<b>-62.34</b>	<b>-56.97</b>
	Our (iv)	1.405	-0.082	-47.01	-46.80	-44.78	-39.21	
	BlowingBubbles	[11]	2.284	-0.146	-54.55	-54.71	-54.47	-57.34
		[12]	1.804	-0.119	-59.73	-59.55	-60.48	-44.02
		[7]	<b>0.611</b>	<b>-0.039</b>	-42.17	-42.64	-43.62	-47.47
		Our (ii)	2.383	-0.151	<b>-62.49</b>	<b>-64.10</b>	<b>-61.00</b>	<b>-59.80</b>
	Our (iv)	0.922	-0.060	-42.03	-43.64	-39.63	-40.93	
	BQSquare	[11]	1.134	-0.083	-54.63	-54.41	-54.10	-53.54
		[12]	1.988	-0.147	-55.97	-60.21	-62.96	-42.92
[7]		1.399	-0.103	-53.52	-56.68	-59.81	<b>-63.04</b>	
Our (ii)		2.035	-0.149	<b>-62.27</b>	<b>-61.45</b>	<b>-64.00</b>	-62.36	
Our (iv)	<b>0.743</b>	<b>-0.054</b>	-42.65	-42.91	-47.02	-45.35		
RaceHorses	[11]	3.416	-0.202	-56.60	-56.23	-55.80	-57.83	
	[12]	2.190	-0.130	-53.50	-54.17	-50.90	-43.34	
	[7]	<b>0.861</b>	<b>-0.051</b>	-41.61	-42.19	-43.71	-43.11	
	Our (ii)	2.917	-0.171	<b>-63.07</b>	<b>-60.96</b>	<b>-60.62</b>	<b>-60.51</b>	
Our (iv)	1.200	-0.071	-41.59	-40.72	-40.76	-43.49		
FourPeople	[11]	3.765	-0.197	-58.59	-56.86	-57.52	-58.52	
	[12]	5.937	-0.307	-66.74	<b>-71.65</b>	<b>-68.51</b>	-62.48	
	[7]	1.336	-0.070	-44.88	-44.41	-40.76	-36.78	
	Our (ii)	3.295	-0.173	<b>-71.63</b>	-68.10	-64.01	<b>-63.88</b>	
Our (iv)	<b>1.334</b>	-0.070	-55.33	-50.24	-45.80	-48.12		
Johnny	[11]	6.479	-0.240	-60.76	-58.49	-57.56	-54.35	
	[12]	6.603	-0.246	-61.68	-62.15	-62.48	<b>-57.19</b>	
	[7]	2.643	-0.098	-49.99	-43.49	-46.12	-43.77	
	Our (ii)	5.084	-0.188	<b>-71.10</b>	<b>-67.32</b>	<b>-62.69</b>	-56.29	
Our (iv)	<b>2.327</b>	<b>-0.087</b>	-54.49	-50.20	-47.19	-40.72		
KristenAndSara	[11]	4.707	-0.215	-58.47	-56.60	-55.88	-53.71	
	[12]	5.413	-0.247	-62.53	-62.12	-61.74	-51.83	
	[7]	2.233	-0.102	-47.86	-43.79	-46.29	-46.29	
	Our (ii)	3.925	-0.181	<b>-73.12</b>	<b>-67.78</b>	<b>-64.36</b>	<b>-59.17</b>	
Our (iv)	<b>1.761</b>	<b>-0.082</b>	-56.50	-51.74	-47.90	-45.73		
Average	[11]	3.443	-0.142	-59.14	-58.70	-57.70	-55.65	
	[12]	4.236	-0.167	-57.02	-64.44	-53.48	-52.48	
	[7]	1.448	-0.060	-38.19	-38.56	-41.79	-40.95	
	Our (ii)	3.188	-0.134	<b>-66.88</b>	<b>-65.67</b>	<b>-63.05</b>	<b>-59.57</b>	
Our (iv)	<b>1.322</b>	<b>-0.055</b>	-47.00	-46.52	-45.08	-44.65		
Standard deviation	[11]	1.352	0.057	<b>3.82</b>	<b>2.34</b>	<b>2.97</b>	<b>5.62</b>	
	[12]	1.692	0.053	4.82	5.45	12.11	8.95	
	[7]	0.553	0.020	9.39	8.87	7.00	7.17	
	Our (ii)	0.915	0.044	4.56	3.03	3.45	8.81	
Our (iv)	<b>0.441</b>	<b>0.017</b>	6.83	4.60	3.66	7.32		

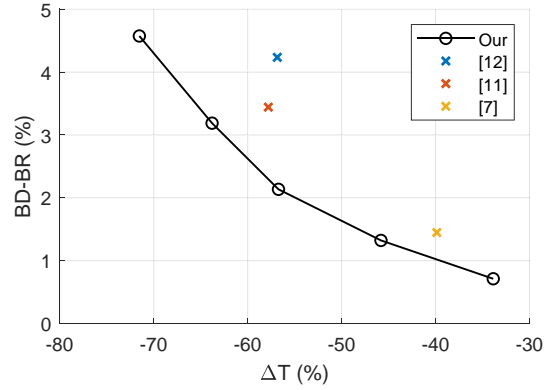


Fig. 6. Complexity-RD performance for our and state-of-the-art approaches.

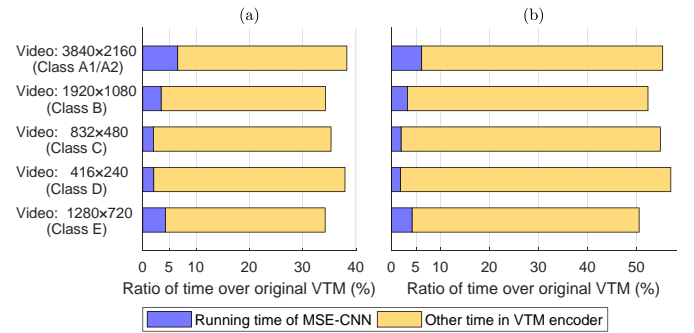


Fig. 7. Running time of the proposed MSE-CNN model and the VTM encoder. (a) Multi-threshold setting of (ii). (b) Multi-threshold setting of (iv).

CU partition. As a result, the total encoding time is averagely reduced by 63.79% and 45.81% at Settings (ii) and (iv) of our approach, respectively, outperforming the state-of-the-art approaches as verified in Section V-B.

## VI. CONCLUSION

In this paper, we have proposed a deep learning approach for fast VVC encoding, through accurately predicting the QTMT-based CU partition at intra-mode. As VVC introduces much more flexible CU partition than HEVC, we first established a large-scale database for learning the diverse patterns of CU partition, and investigated the available split modes of CUs on multiple stages. Next, we proposed a deep MSE-CNN model to determine the CU partition, combining the conditional convolution and sub-networks with sufficient network capacity. Then, we designed an early exit mechanism for the MSE-CNN model, which can skip the redundant checking processes on un-used CUs. Moreover, a multi-threshold decision scheme was developed, achieving a desirable trade-off between encoding complexity and RD performance. The experimental results show that our approach can averagely save the encoding time by 44.65%~66.88% with the negligible 1.322%~3.188% of BD-BR increase on video sequences, outperforming other state-of-the-art approaches.

For future works, the encoding time of inter-mode VVC can also be saved with deep learning. Besides accelerating the CU partition, there exists a potential to accelerate other processes in VVC, e.g., intra-angular selection and motion vector

estimation, with properly designed deep neural networks. In addition, our approach may be further sped up with various network acceleration techniques or implementation on field programmable gate array (FPGA) device. This can be seen as another promising work for facilitating fast VVC encoders in the coming years.

## REFERENCES

- [1] Joint Video Experts Team (JVET), "VTM Software," [Online]. Available: [https://vcgit.hhi.fraunhofer.de/jvet/VVCSofware\\_VTM/](https://vcgit.hhi.fraunhofer.de/jvet/VVCSofware_VTM/), 2020, [Accessed 23-Feb.-2020].
- [2] J. Leng, L. Sun, T. Ikenaga, and S. Sakaida, "Content based hierarchical fast coding unit decision algorithm for HEVC," in *International Conference on Multimedia and Signal Processing (ICMSP)*, vol. 1, 2011, pp. 56–59.
- [3] L. Shen, Z. Zhang, and Z. Liu, "Effective CU size decision for HEVC intracoding," *IEEE Transactions on Image Processing (TIP)*, vol. 23, no. 10, pp. 4232–4241, Oct. 2014.
- [4] Y. Zhang, S. Kwong, X. Wang, H. Yuan, Z. Pan and L. Xu, "Machine learning-based coding unit depth decisions for flexible complexity allocation in high efficiency video coding," *IEEE Transactions on Image Processing (TIP)*, vol. 24, no. 7, pp. 2225–2238, Jul. 2015.
- [5] L. Zhu, Y. Zhang, Z. Pan, R. Wang, S. Kwong and Z. Peng, "Binary and multi-class learning based low complexity optimization for HEVC encoding," *IEEE Transactions on Broadcasting (TBC)*, pp. 1–15, Jun. 2017.
- [6] Z. Liu, X. Yu, Y. Gao, S. Chen, X. Ji, and D. Wang, "CU partition mode decision for HEVC hardwired intra encoder using convolution neural network," *IEEE Transactions on Image Processing (TIP)*, vol. 25, no. 11, pp. 5088–5103, Nov. 2016.
- [7] M. Xu, T. Li, Z. Wang, X. Deng, R. Yang, and Z. Guan, "Reducing complexity of HEVC: A deep learning approach," *IEEE Transactions on Image Processing*, vol. 27, no. 10, pp. 5044–5059, Oct 2018.
- [8] T. I. Y. Yamamoto, "Ahg5: Fast qtbt encoding configuration," *JVET-D0095, Joint Video Exploration Team (JVET)*, vol. 27, no. 10, pp. 5044–5059, 2016.
- [9] W. Zhao, S. Wang, Z. Jian, S. Wang, and S. Ma, "Effective quadtree plus binary tree block partition decision for future video coding," in *Data Compression Conference, 2017*.
- [10] T. Amestoy, A. Mercat, W. Hamidouche, C. Bergeron, and D. Menard, "Random forest oriented fast QTBT frame partitioning," in *IEEE International Conference on Acoustics, Speech and Signal Processing (ICASSP)*, May 2019, pp. 1837–1841.
- [11] T. Fu, H. Zhang, F. Mu, and H. Chen, "Fast cu partitioning algorithm for h.266/vvc intra-frame coding," in *2019 IEEE International Conference on Multimedia and Expo (ICME)*, July 2019, pp. 55–60.
- [12] H. Yang, L. Shen, X. Dong, Q. Ding, P. An, and G. Jiang, "Low complexity ctu partition structure decision and fast intra mode decision for versatile video coding," *IEEE Transactions on Circuits and Systems for Video Technology*, pp. 1–1, 2019.
- [13] Z. Jin, P. An, L. Shen, and C. Yang, "Cnn oriented fast qtbt partition algorithm for jvet intra coding," in *IEEE Visual Communications and Image Processing (VCIP)*, Dec 2017, pp. 1–4.
- [14] Z. Wang, S. Wang, X. Zhang, S. Wang, and S. Ma, "Fast qtbt partitioning decision for interframe coding with convolution neural network," in *IEEE International Conference on Image Processing (ICIP)*, Oct 2018, pp. 2550–2554.
- [15] F. Galpin, F. Racap, S. Jaiswal, P. Bordes, F. Le Lannec, and E. Franois, "Cnn-based driving of block partitioning for intra slices encoding," in *2019 Data Compression Conference (DCC)*, March 2019, pp. 162–171.
- [16] D. Mukherjee, J. Bankoski, A. Grange, J. Han, J. Koleszar, P. Wilkins, Y. Xu, and R. Bultje, "The latest open-source video codec vp9 - an overview and preliminary results," in *2013 Picture Coding Symposium (PCS)*, Dec 2013, pp. 390–393.
- [17] Y. Chen, D. Murherjee, J. Han, A. Grange, Y. Xu, Z. Liu, S. Parker, C. Chen, H. Su, U. Joshi, C. Chiang, Y. Wang, P. Wilkins, J. Bankoski, L. Trudeau, N. Egge, J. Valin, T. Davies, S. Midtskogen, A. Norkin, and P. de Rivaz, "An overview of core coding tools in the av1 video codec," in *2018 Picture Coding Symposium (PCS)*, June 2018, pp. 41–45.
- [18] Z. He, L. Yu, X. Zheng, S. Ma, and Y. He, "Framework of avs2-video coding," in *IEEE International Conference on Image Processing*, Sep. 2013, pp. 1515–1519.
- [19] J. Xiong, H. Li, Q. Wu, and F. Meng, "A fast HEVC inter CU selection method based on pyramid motion divergence," *IEEE Transactions on Multimedia (TMM)*, vol. 16, no. 2, pp. 559–564, Feb. 2014.
- [20] S. Cho and M. Kim, "Fast CU splitting and pruning for suboptimal CU partitioning in HEVC intra coding," *IEEE Transactions on Circuits and Systems for Video Technology (TSCVT)*, vol. 23, no. 9, pp. 1555–1564, Sept. 2013.
- [21] X. Shen, L. Yu and J. Chen, "Fast coding unit size selection for HEVC based on Bayesian decision rule," in *Picture Coding Symposium (PCS)*, 2012.
- [22] N. Kim, S. Jeon, H. J. Shim, B. Jeon, S. C. Lim and H. Ko, "Adaptive keypoint-based CU depth decision for HEVC intra coding," in *IEEE International Symposium on Broadband Multimedia Systems and Broadcasting (BMSB)*, 2016.
- [23] B. Min and R. C. C. Cheung, "A fast cu size decision algorithm for the hevc intra encoder," *IEEE Transactions on Circuits and Systems for Video Technology*, vol. 25, no. 5, pp. 892–896, 2015.
- [24] Y. Zhang, S. Kwong, G. Jiang, X. Wang, and M. Yu, "Statistical early termination model for fast mode decision and reference frame selection in multiview video coding," *IEEE Transactions on Broadcasting*, vol. 58, no. 1, pp. 10–23, 2012.
- [25] G. Corrêa, P. A. Assuncao, L. V. Agostini and L. A. da Silva Cruz, "Fast HEVC encoding decisions using data mining," *IEEE Transactions on Circuits and Systems for Video Technology (TCSVT)*, vol. 25, no. 4, pp. 660–673, Apr. 2015.
- [26] Q. Hu, Z. Shi, X. Zhang and Z. Gao, "Fast HEVC intra mode decision based on logistic regression classification," in *IEEE International Symposium on Broadband Multimedia Systems and Broadcasting (BMSB)*, 2016.
- [27] Q. Hu, X. Zhang, Z. Shi, and Z. Gao, "Neyman-pearson based early mode decision for hevc encoding," *IEEE Transactions on Multimedia*, vol. 18, no. 3, pp. 379–391, 2016.
- [28] D. Liu, X. Liu and Y. Li, "Fast CU size decisions for HEVC intra frame coding based on support vector machines," in *2016 IEEE 14th Intl Conf on Dependable, Autonomic and Secure Computing (DASC)*, 2016.
- [29] M. Alencar and J. de Oliveira, "Online learning early skip decision method for the hevc inter process using the svm-based pegasos algorithm," *Electronics Letters*, vol. 52, no. 14, pp. 1227–1229, 2016.
- [30] F. Duanmu, Z. Ma, and Y. Wang, "Fast mode and partition decision using machine learning for intra-frame coding in hevc screen content coding extension," *IEEE Journal on Emerging and Selected Topics in Circuits and Systems*, vol. 6, no. 4, pp. 517–531, Dec 2016.
- [31] S. Momcilovic, N. Roma, L. Sousa, and I. Milentjevic, "Run-time machine learning for HEVC/H.265 fast partitioning decision," in *IEEE International Symposium on Multimedia*, 2015.
- [32] B. Du, W. Siu, and X. Yang, "Fast cu partition strategy for hevc intra-frame coding using learning approach via random forests," in *2015 Asia-Pacific Signal and Information Processing Association Annual Summit and Conference (APSIPA)*, Dec 2015, pp. 1085–1090.
- [33] Y. Shan and E. Yang, "Fast hevc intra coding algorithm based on machine learning and laplacian transparent composite model," in *2017 IEEE International Conference on Acoustics, Speech and Signal Processing (ICASSP)*, March 2017, pp. 2642–2646.
- [34] X. Shen and L. Yu, "Cu splitting early termination based on weighted svm," *Eurasip Journal on Image and Video Processing*, vol. 2013, no. 1, p. 4, 2013.
- [35] N. Westland, A. S. Dias, and M. Mrak, "Decision trees for complexity reduction in video compression," in *2019 IEEE International Conference on Image Processing (ICIP)*, Sep. 2019, pp. 2666–2670.
- [36] M. U. K. Khan, M. Shafique and J. Henkel, "An adaptive complexity reduction scheme with fast prediction unit decision for HEVC intra encoding," in *2013 IEEE International Conference on Image Processing*, 2013.
- [37] H. M. Yoo and J. W. Suh, "Fast coding unit decision algorithm based on inter and intra prediction unit termination for HEVC," in *2013 IEEE International Conference on Consumer Electronics (ICCE)*, 2013.
- [38] W. Jiang, H. Ma, and Y. Chen, "Gradient based fast mode decision algorithm for intra prediction in hevc," in *International Conference on Consumer Electronics*, 2012.
- [39] L. L. Wang and W. C. Siu, "Novel adaptive algorithm for intra prediction with compromised modes skipping and signaling processes in hevc," *IEEE Transactions on Circuits and Systems for Video Technology*, vol. 23, no. 10, pp. 1686–1694, 2013.
- [40] J. Lei, D. Li, Z. Pan, Z. Sun, S. Kwong, and C. Hou, "Fast intra prediction based on content property analysis for low complexity hevc-based screen content coding," *IEEE Transactions on Broadcasting*, vol. 63, no. 1, pp. 48–58, 2017.

- [41] J. Cui, S. Wang, S. Wang, X. Zhang, S. Ma and W. Gao, "Hybrid Laplace distribution-based low complexity rate-distortion optimized quantization," *IEEE Transactions on Image Processing*, vol. 26, no. 8, pp. 3802–3816, Aug 2017.
- [42] Z. Liu, X. Yu, S. Chen, and D. Wang, "Cnn oriented fast hevc intra cu mode decision," in *IEEE International Symposium on Circuits and Systems*, 2016.
- [43] T. Laude and Ostermann, "Deep learning-based intra prediction mode decision for hevc," in *Picture Coding Symposium*, 2017.
- [44] S. Paul, A. Norkin, and A. C. Bovik, "Speeding up vp9 intra encoder with hierarchical deep learning based partition prediction," in *AOMedia 2019 Research Symposium (AOMRS)*, 2019.
- [45] H. Su, C. Tsai, Y. Wang, and Y. Xu, "Machine learning accelerated partition search for video encoding," in *2019 IEEE International Conference on Image Processing (ICIP)*, Sep. 2019, pp. 2661–2665.
- [46] W. Lin, Z. Liu, D. Mukherjee, J. Han, P. Wilkins, Y. Xu, and K. Rose, "Efficient av1 video coding using a multi-layer framework," in *2018 Data Compression Conference (DCC)*, March 2018, pp. 365–373.
- [47] C. Chiang, J. Han, and Y. Xu, "A multi-pass coding mode search framework for av1 encoder optimization," in *Data Compression Conference (DCC)*, March 2019, pp. 458–467.
- [48] J. Kim, S. Blasi, A. S. Dias, M. Mrak, and E. Izquierdo, "Fast inter-prediction based on decision trees for av1 encoding," in *IEEE International Conference on Acoustics, Speech and Signal Processing (ICASSP)*, May 2019, pp. 1627–1631.
- [49] J. Li, F. Luo, Y. Zhou, S. Wang, M. Wang, and S. Ma, "Content based fast intra coding for avs2," in *IEEE Third International Conference on Multimedia Big Data (BigMM)*, April 2017, pp. 94–97.
- [50] H. Xie, G. Xiang, D. Yu, H. Yu, Y. Li, and W. Yan, "Perceptual fast cu size decision algorithm for avs2 intra coding," in *IEEE Fifth International Conference on Multimedia Big Data (BigMM)*, Sep. 2019, pp. 277–281.
- [51] M. Yuan, Y. Xue, S. Ohn, and S. Hyung, "Fast cu size and pu partition decision for avs2 intra coding," in *IEEE International Symposium on Broadband Multimedia Systems and Broadcasting (BMSB)*, June 2018, pp. 1–5.
- [52] X. Liu, W. Yan, G. Xiang, L. Cheng, and Y. Yan, "A novel fast mode decision algorithm for avs2 intra coding," in *International Conference on Signal and Image Processing (ICSIP)*, July 2019, pp. 850–854.
- [53] T. Amestoy, A. Mercat, W. Hamidouche, D. Menard, and C. Bergeron, "Tunable vvc frame partitioning based on lightweight machine learning," *IEEE Transactions on Image Processing*, vol. 29, pp. 1313–1328, 2020.
- [54] M. Lei, F. Luo, X. Zhang, S. Wang, and S. Ma, "Look-ahead prediction based coding unit size pruning for VVC intra coding," in *IEEE International Conference on Image Processing (ICIP)*, Sep. 2019, pp. 4120–4124.
- [55] K. He, X. Zhang, S. Ren, and J. Sun, "Deep residual learning for image recognition," in *2016 IEEE CVPR*, June 2016, pp. 770–778.
- [56] D.-T. Dang-Nguyen, C. Pasquini, V. Conotter, and G. Boato, "RAISE: A raw images dataset for digital image forensics," in *Proceedings of the 6th ACM Multimedia Systems Conference*, 2015, pp. 219–224.
- [57] M. Xu, X. Deng, S. Li and Z. Wang, "Region-of-interest based conversational HEVC coding with hierarchical perception model of face," *IEEE JSTSP*, vol. 8, no. 3, pp. 475–489, Jun. 2014.
- [58] CDVL.org, "Consumer digital video library," <https://www.cdvl.org>, 2019.
- [59] Xiph.org, "Xiph.org video test media," <https://media.xiph.org/video/derf>, 2017.
- [60] J. Boyce, K. Suehring, X. Li and V. Seregin, "JVET common test conditions and software reference configurations," in *JVET-J1010, San Diego, US*, Apr. 2018.
- [61] K. He, X. Zhang, S. Ren and J. Sun, "Delving deep into rectifiers: Surpassing human-level performance on ImageNet classification," in *2015 IEEE ICCV*, Dec 2015, pp. 1026–1034.
- [62] G. Bjøntegaard, "Calculation of average PSNR difference between RD-curves," in *ITU-T, VCEG-M33, Austin, TX, USA*, Apr. 2001.
- [63] X. Glorot and Y. Bengio, "Understanding the difficulty of training deep feedforward neural networks," in *AISTATS*, vol. 9, 2010, pp. 249–256.
- [64] D. P. Kingma and J. Ba, "Adam: A method for stochastic optimization," *Computer Science*, 2014.